# micromagnetism
# nanomagnetism

---

an

MMM mini-lecture

by

Willem van Engen

on

October 24, 2007

---

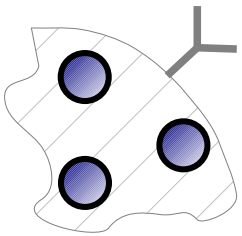

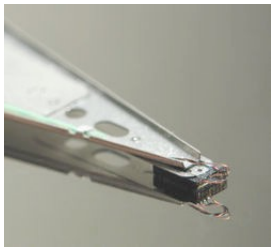

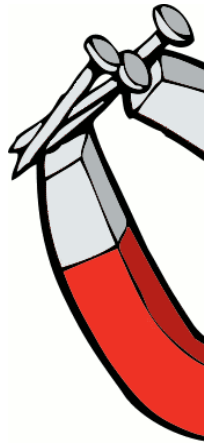

0 nm µm cm

# Crucial Experiment Demonstrating Single Domain Property of Fine Ferromagnetic Powders

C. KITTEL, J. K. GALT AND W. E. CAMPBELL
*Bell Telephone Laboratories, Murray Hill, New Jersey*
January 18, 1950




IT is now well known that fine ferromagnetic powders have high coercivities and this has been explained on the supposition that a sufficiently fine particle will consist of a single magnetic domain, as suggested by domain theory. The objection is sometimes raised that it might be possible to explain the high coercivity without the single-domain assumption, by supposing that internal strains are very large in fine powders, and that the strains hinder and retard magnetization changes by domain boundary displacement, thereby giving high coercivity. It may seem difficult to prove that the internal strain hypothesis will not account for the observed corecivities of 200 and 600 oersteds in fine nickel and iron powder, although it appears most improbable that strains are responsible for the unusually high coercivities observed in fine powders of MnBi ($H_c = 12{,}000$ oersteds) and FePt ($H_c = 20{,}000$ oersteds).

doi:10.1103/PhysRev.77.725

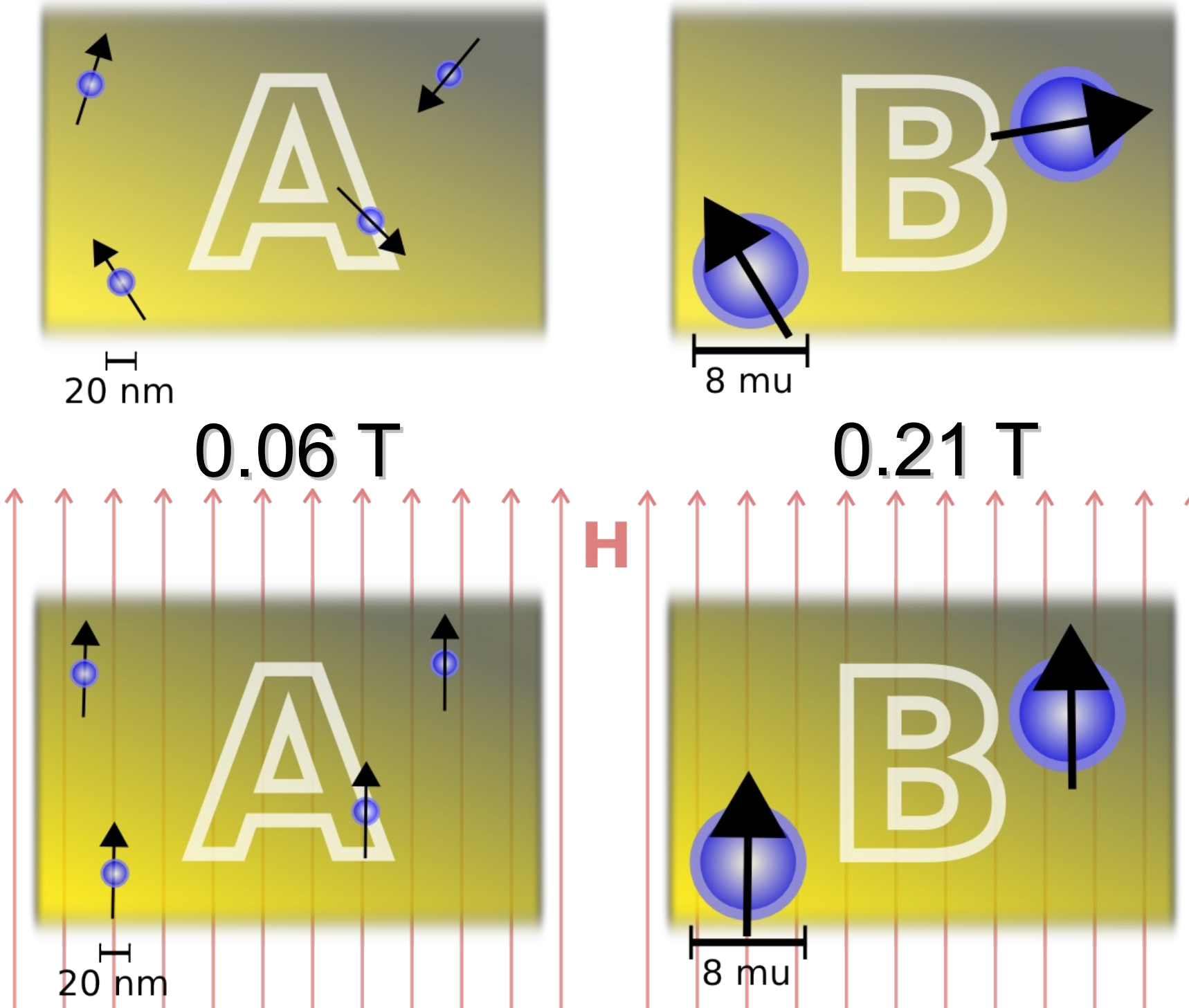
A
B
20 nm
8 mu
0.06 T
0.21 T
H
A
B
20 nm
8 mu

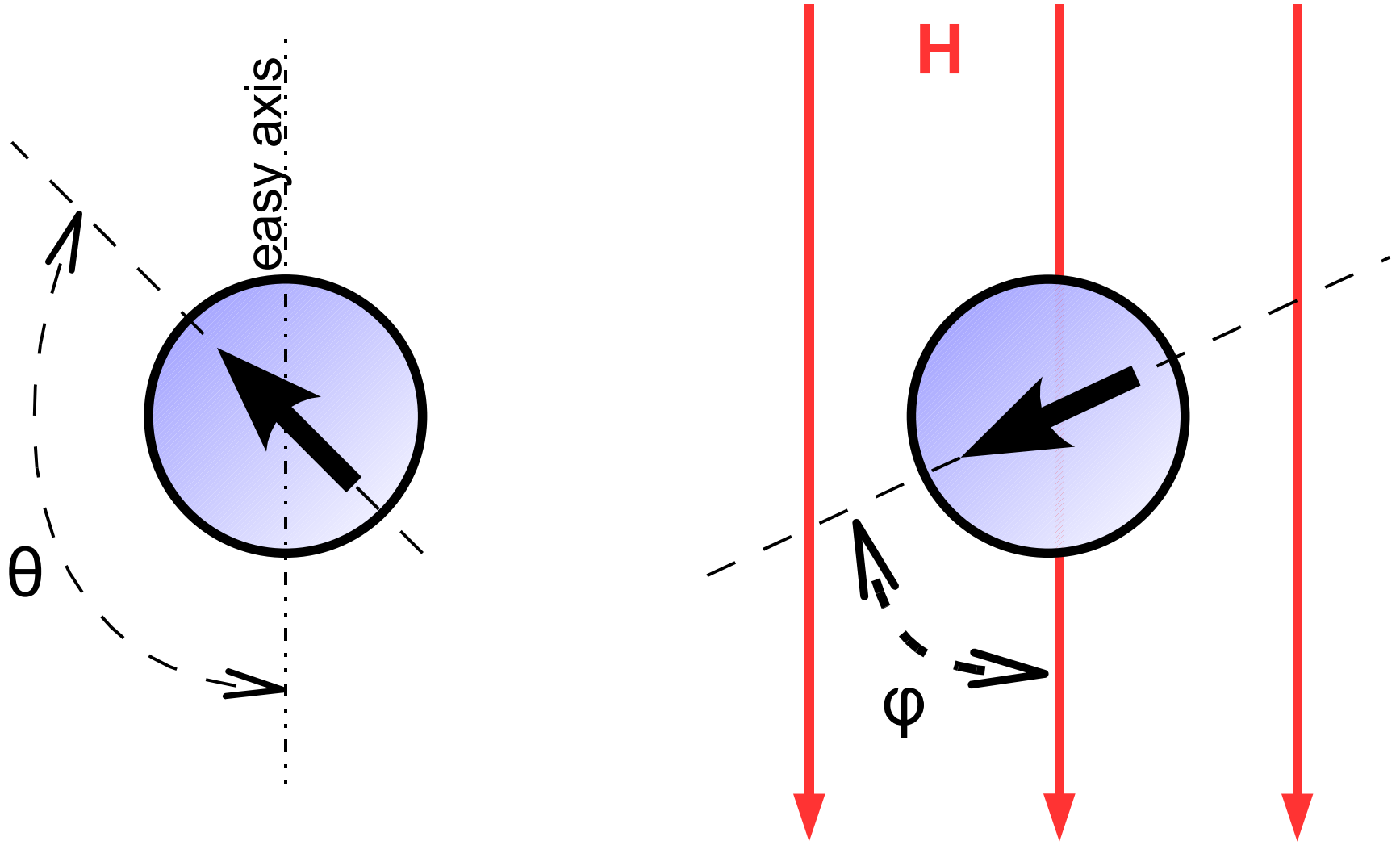
easy axis
θ
H
φ

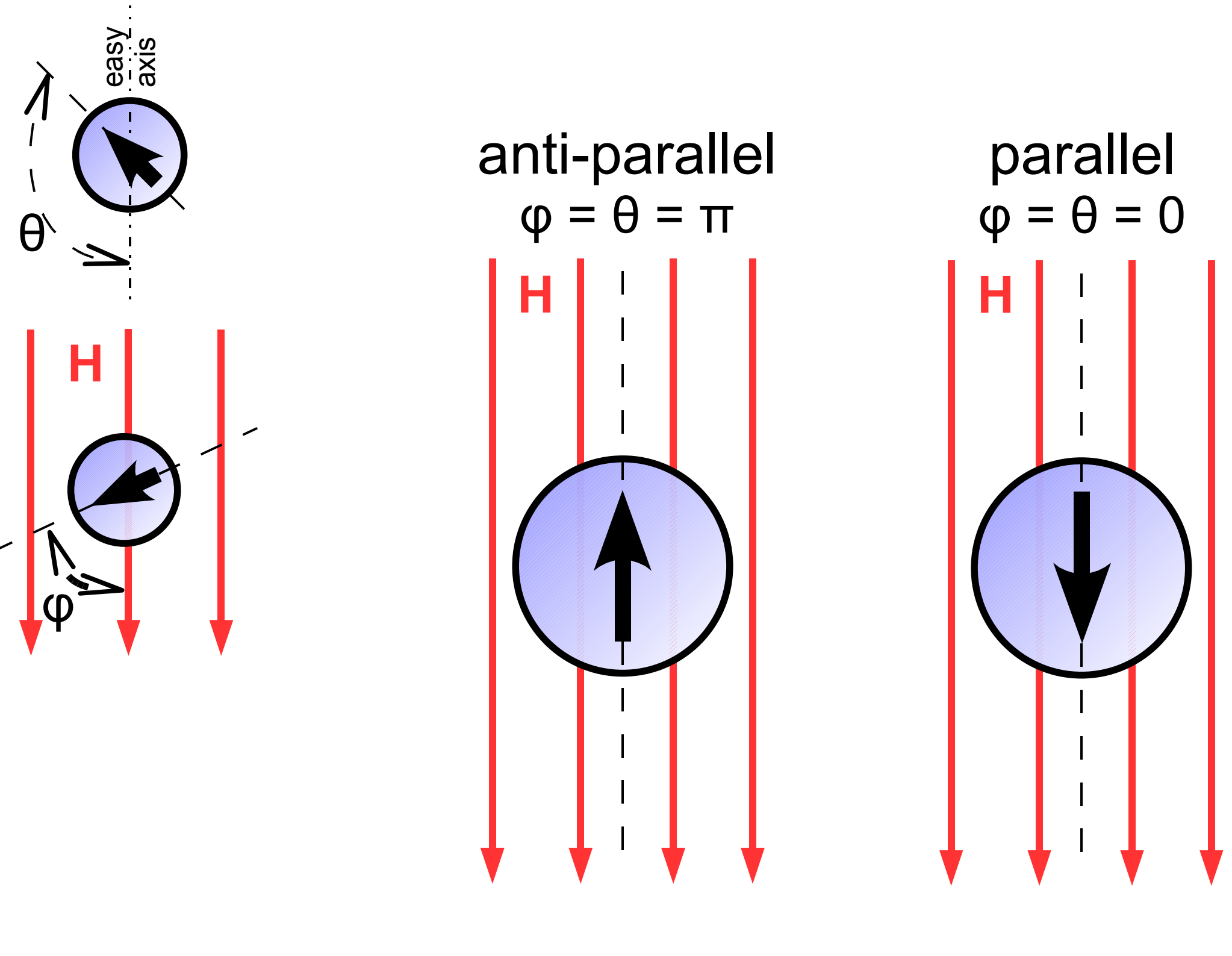
easy axis
θ
H
φ
anti-parallel
φ = θ = π
H
parallel
φ = θ = 0
H

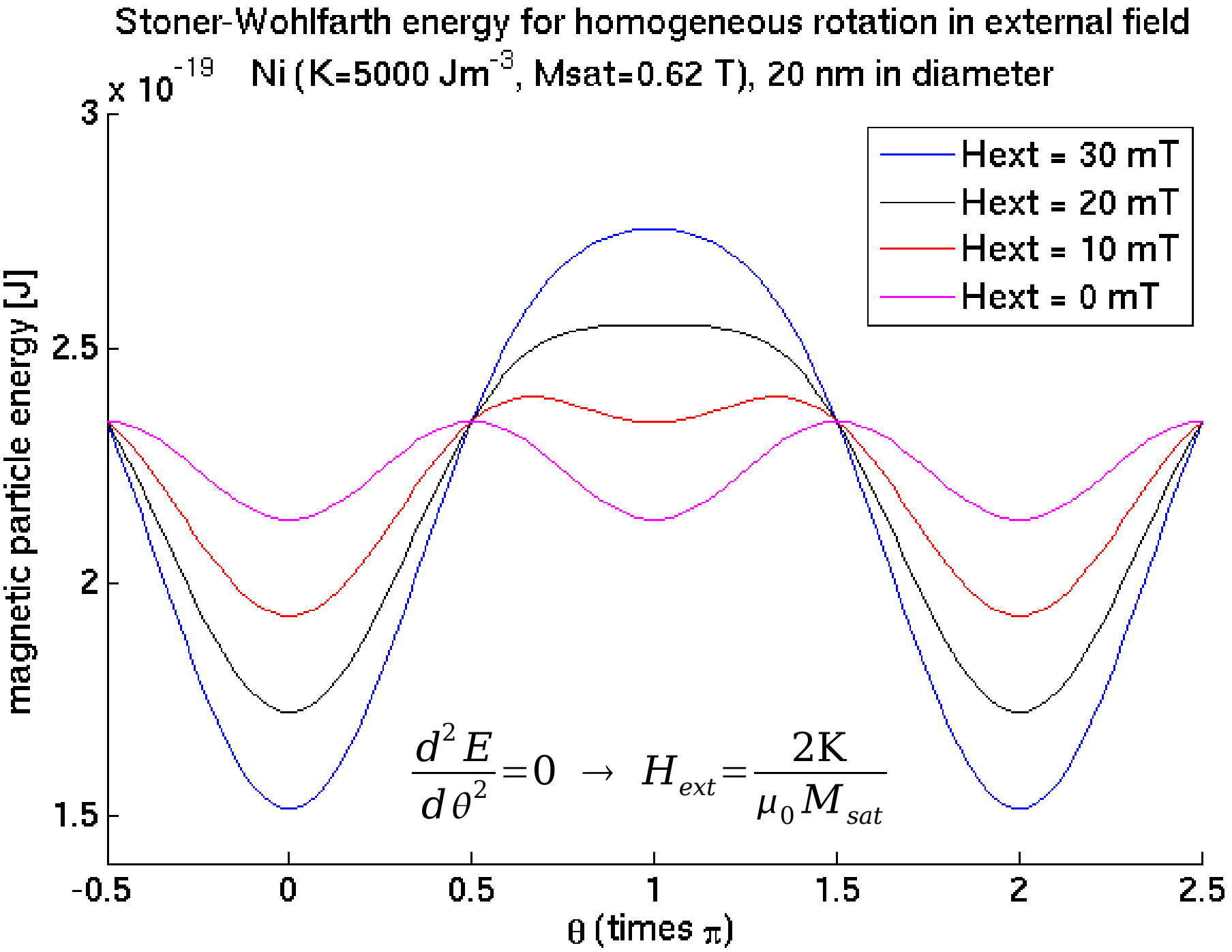
Stoner-Wohlfarth energy for homogeneous rotation in external field
Ni (K=5000 Jm^-3, Msat=0.62 T), 20 nm in diameter
x 10^-19
magnetic particle energy [J]
3
2.5
2
1.5
-0.5
0
0.5
1
1.5
2
2.5
θ (times π)
Hext = 30 mT
Hext = 20 mT
Hext = 10 mT
Hext = 0 mT
$\frac{d^2E}{d\theta^2}=0 \rightarrow H_{ext}=\frac{2K}{\mu_0 M_{sat}}$

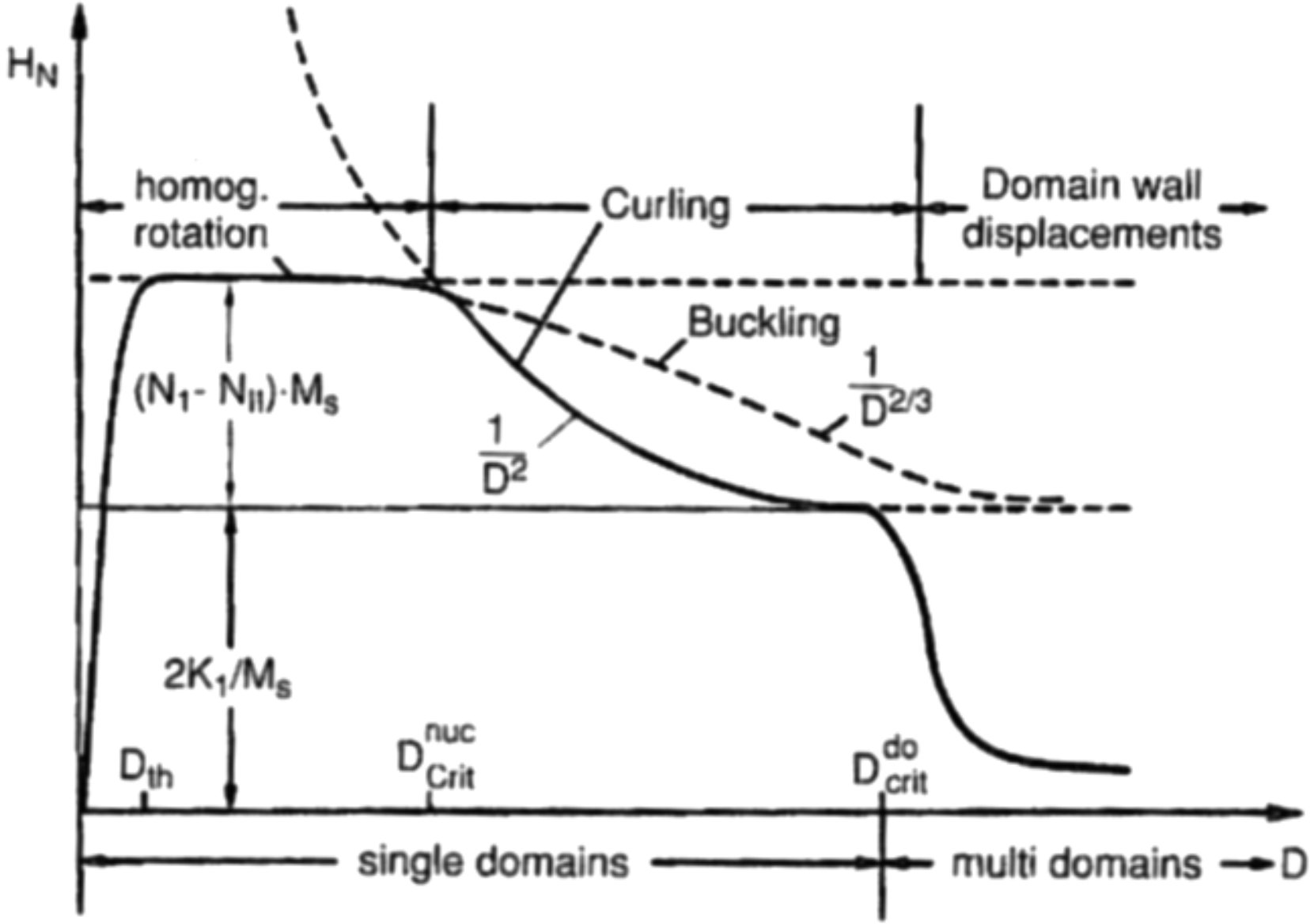


Fig. 6.12. Review of the nucleation fields of different hardening mechanisms. Critical diameters are discussed in Section 6.2.4.

"Micromagnetism and the Microstructure of Ferromagnetic solids", Kronmüller and Fahnle, 2003. ISBN 0521331358

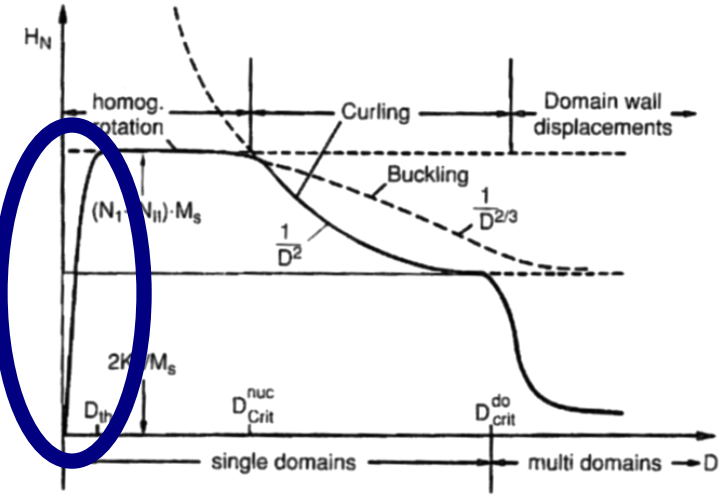


# superparamagnetism

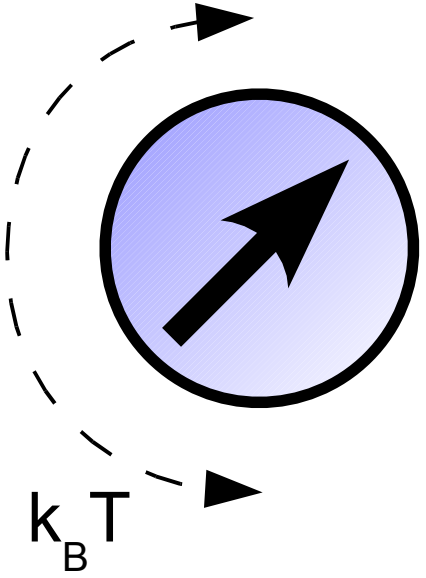


$$D_{th}{}^3 = \frac{6 k_B T}{\pi K} \ln \frac{\tau_m}{\tau_0}$$

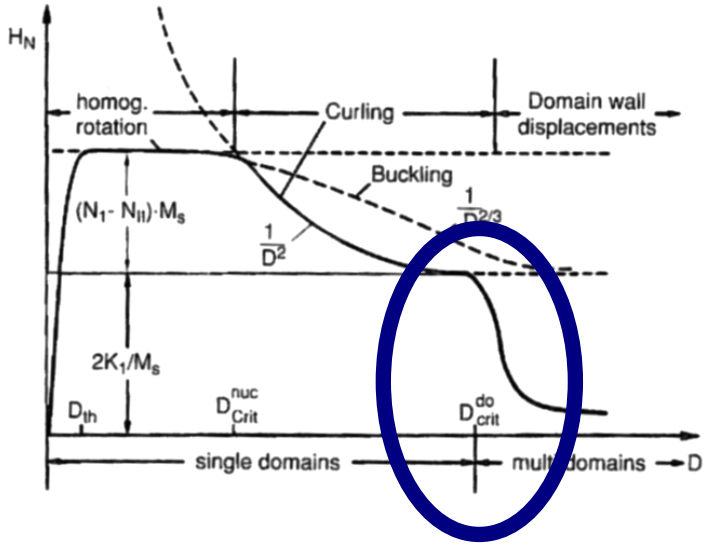


# single vs. multi domain

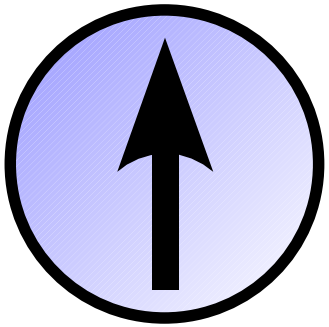

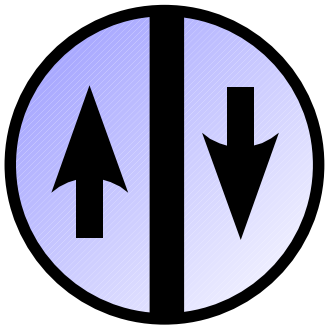

$$D_{do} = \frac{18\gamma}{\mu_0 M_{sat}^{\ 2}}$$

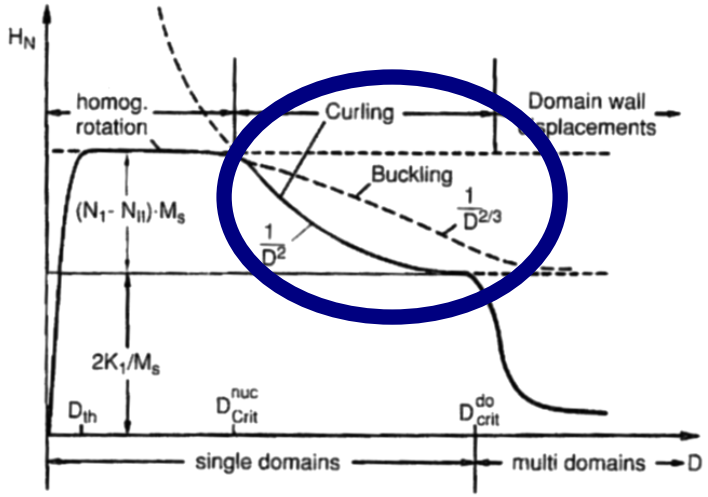


# curling ...

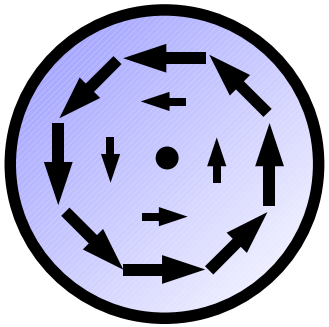

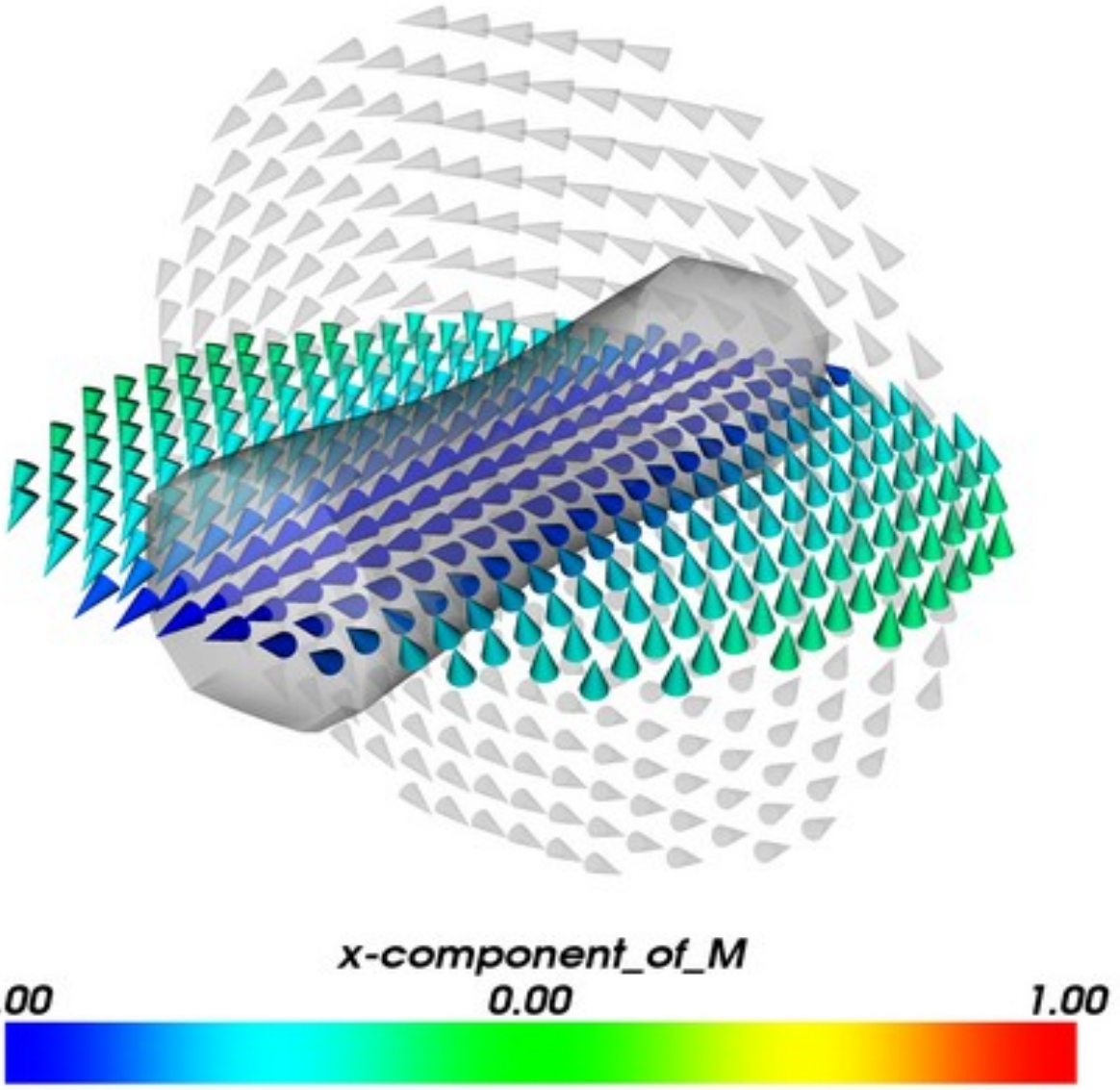


"Micromagnetism", Boardman, 2006. http://www.soton.ac.uk/~rpb/

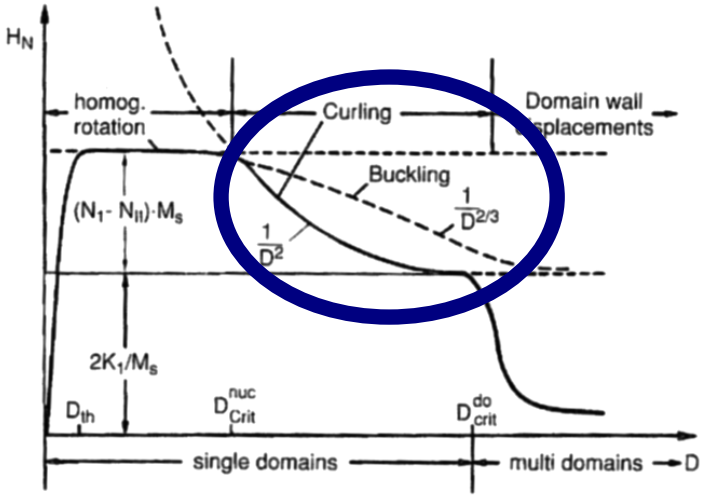


# ... or buckling

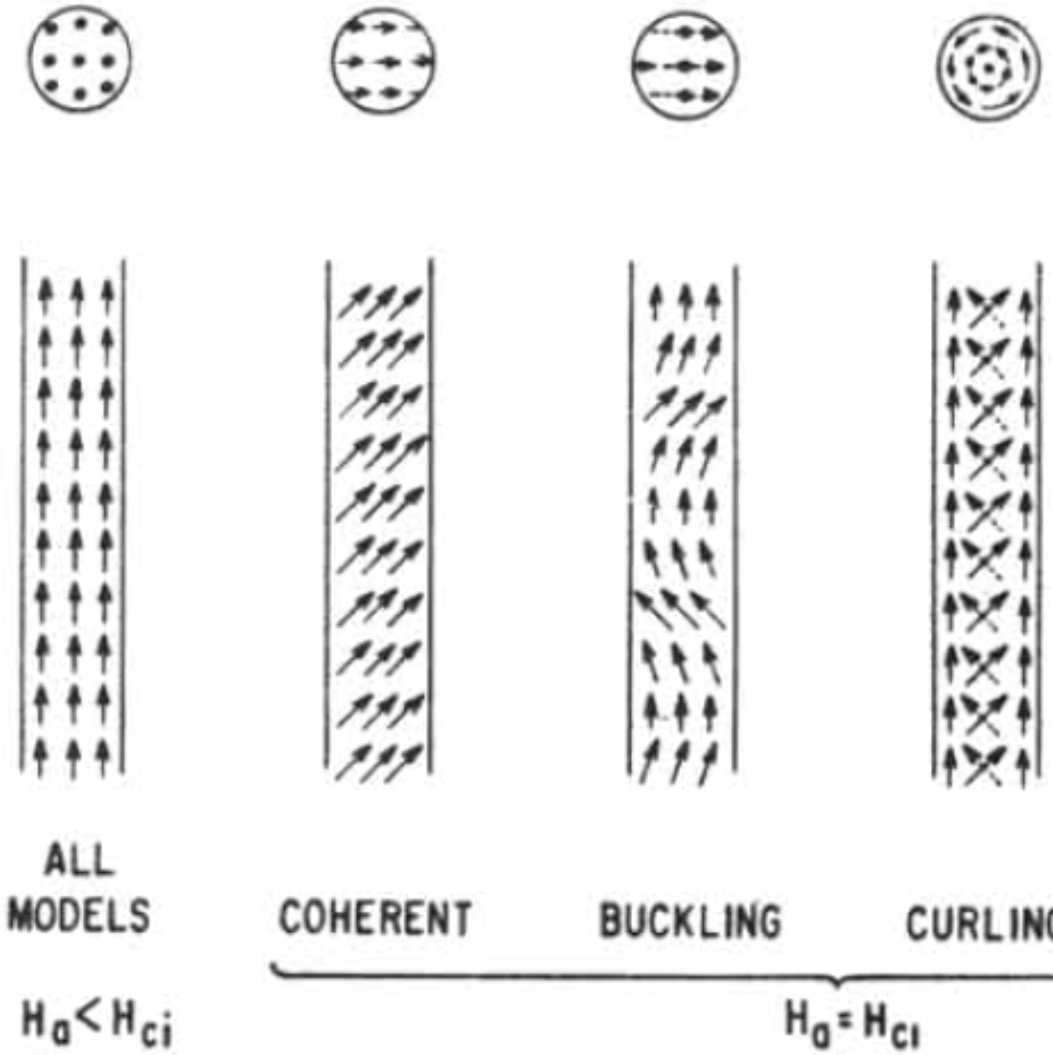


"Development of elongated particle magnets", Luborsky, 1961. doi:10.1063/1.2000392

**Co:**

**Fe:**

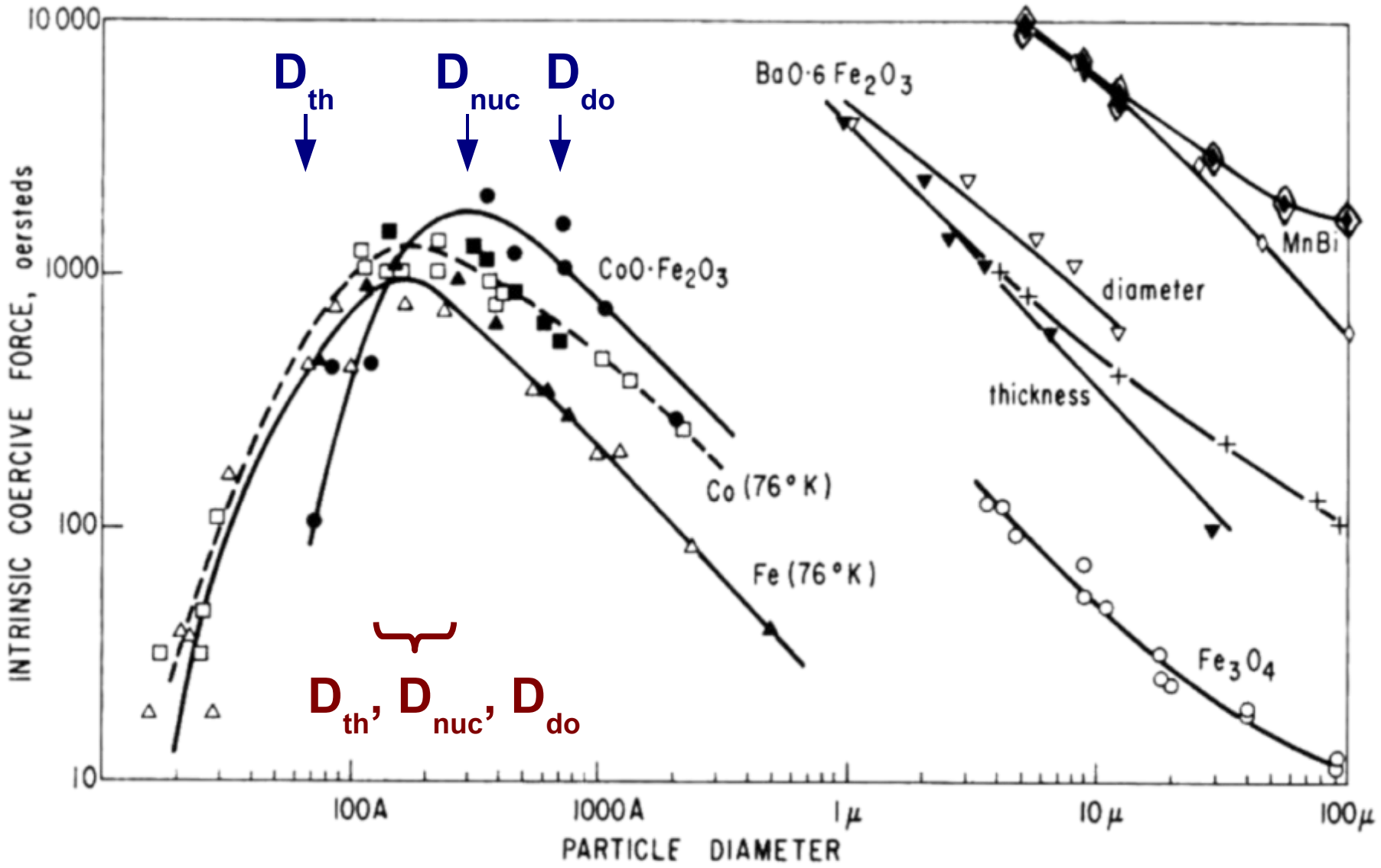


FIG. 2. Experimental relation between diameter and coercive force for particles deriving their coercive force principally from crystal anisotropy energy. All measured at room temperature except Co and Fe. MnBi, ◇ Guillaud [C. Guillaud, thesis, University of Strasbourg (1943)], ◈ Shur [Ia. S. Shur, Trudy Inst. Fiz. Metall. Akad. Nauk S.S.S.R. **20**, 111 (1958)]; $BaO \cdot 6Fe_2O_3$, ▽ ▼ Sixtus *et al.* [K. J. Sixtus, K. J. Kronenberg, and R. K. Tenzer, J. Appl. Phys. **27**, 1051 (1956)], + Brockman [F. G. Brockman, Eighth Progress Report, Signal Corps Project No. 32-2005D (1955)]; $Fe_3O_4$, ○ Gottschalk, see footnote 5; $CoO \cdot Fe_2O_3$, ● Berkowitz and Schuele [A. Berkowitz and W. Schuele, J. Appl. Phys. **30**, 134S (1959)]; Co, ■ Meiklejohn [W. H. Meiklejohn, Revs. Modern Phys. **25**, 302 (1953)], □ Luborsky [F. E. Luborsky (to be published)]; Fe, ▲ Meiklejohn [W. H. Meiklejohn, Revs. Modern Phys. **25**, 302 (1953)], △ Luborsky and Paine [F. E. Luborsky and T. O. Paine, J. Appl. Phys. **31**, 68S (1960) and an article to be published.

"Development of elongated particle magnets", Luborsky, 1961. doi:10.1063/1.2000392

**enough theory**

**applications!**

# microfluidics ...

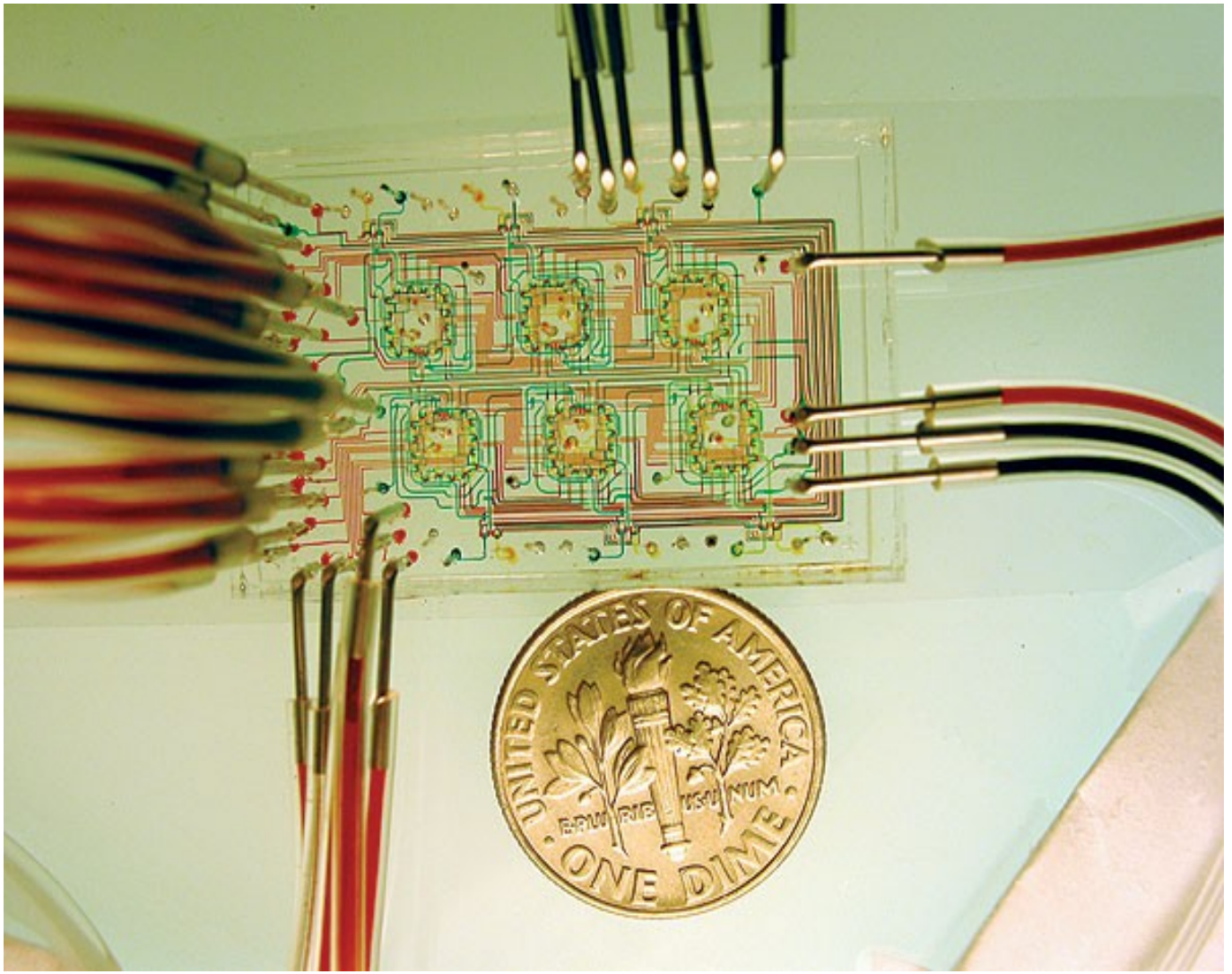


"The origins and the future of microfluidics", Whitesides, 2006. doi:10.1038/nature05058

# **microfluidics ...**
ferrofluidics

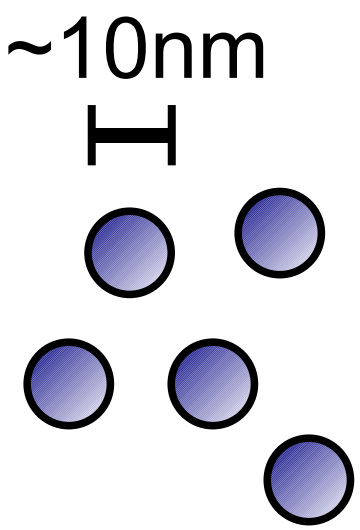


+

=

source: Technorama

# **microfluidics ...**
ferrofluidic pump

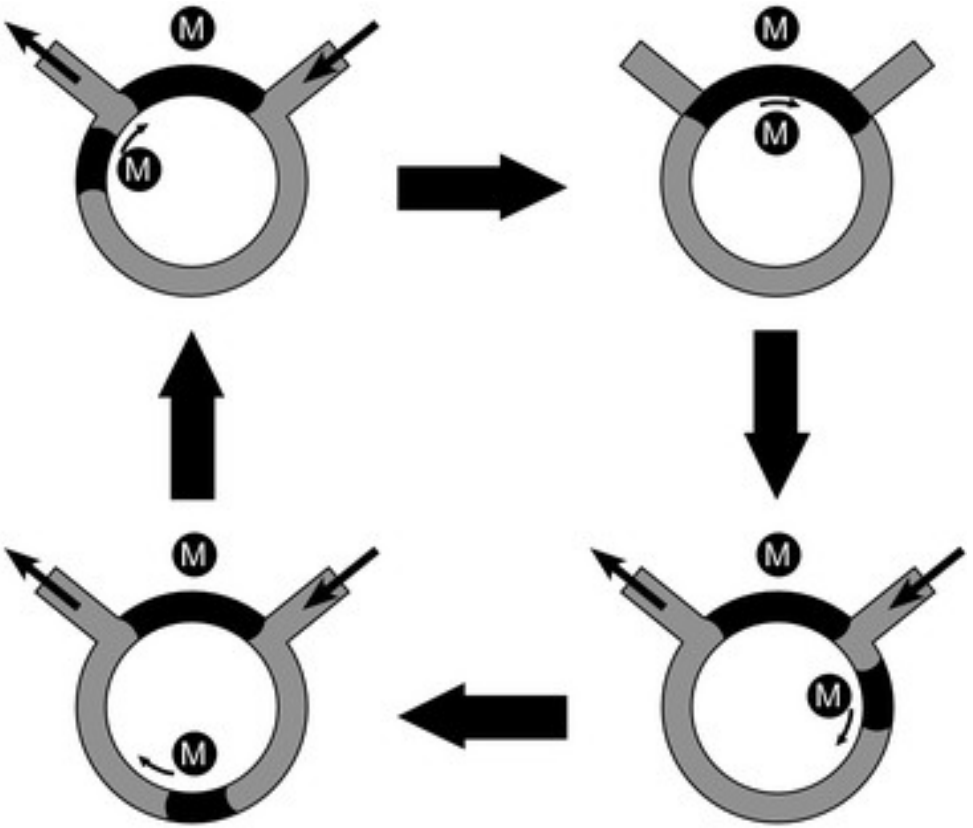


“Magnetism and microfluidics”, Pamme, 2006. doi:10.1039/b513005k

# **biosensors**
## magnetic bead

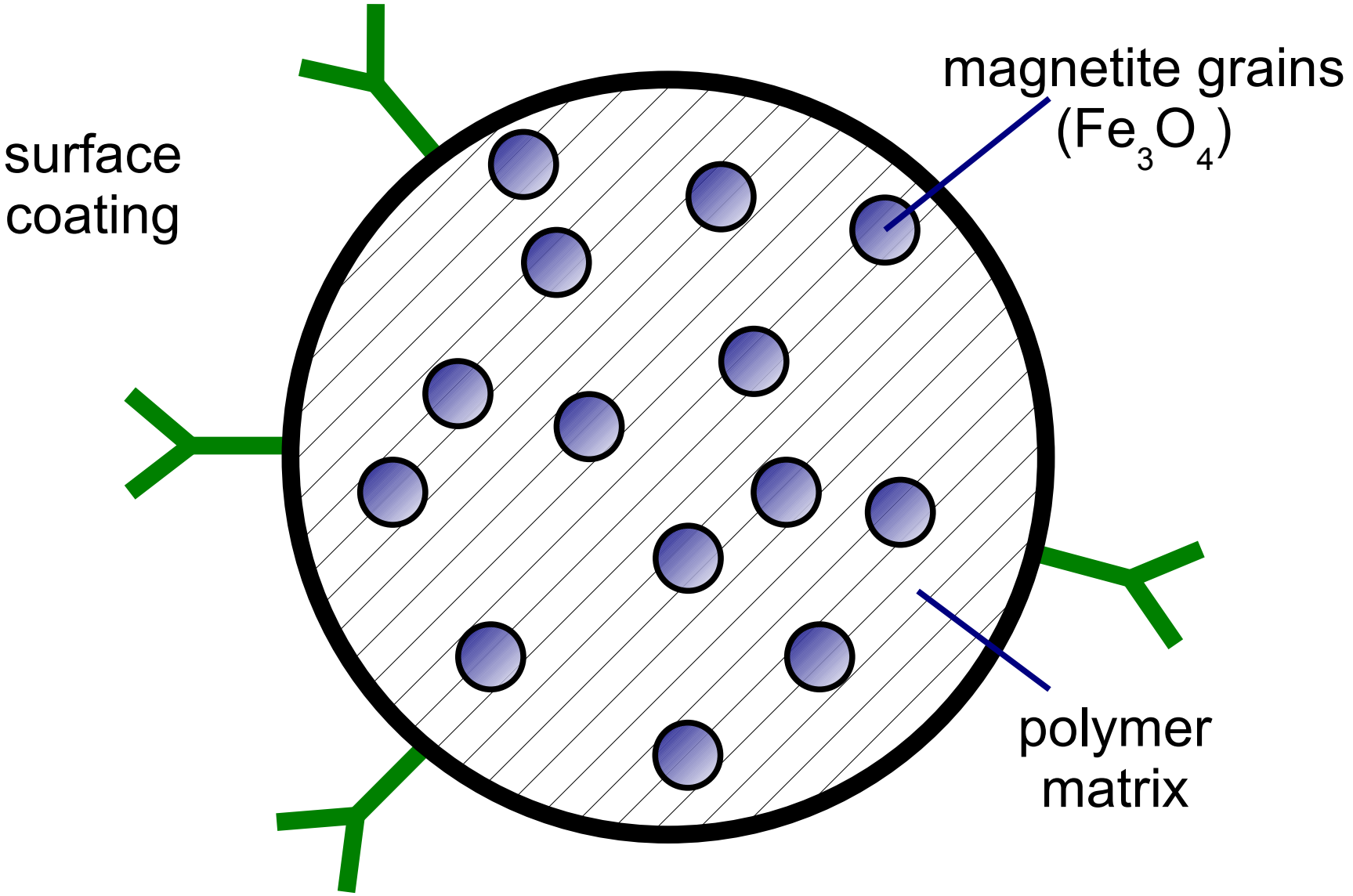

# **biosensors**
biochemical binding

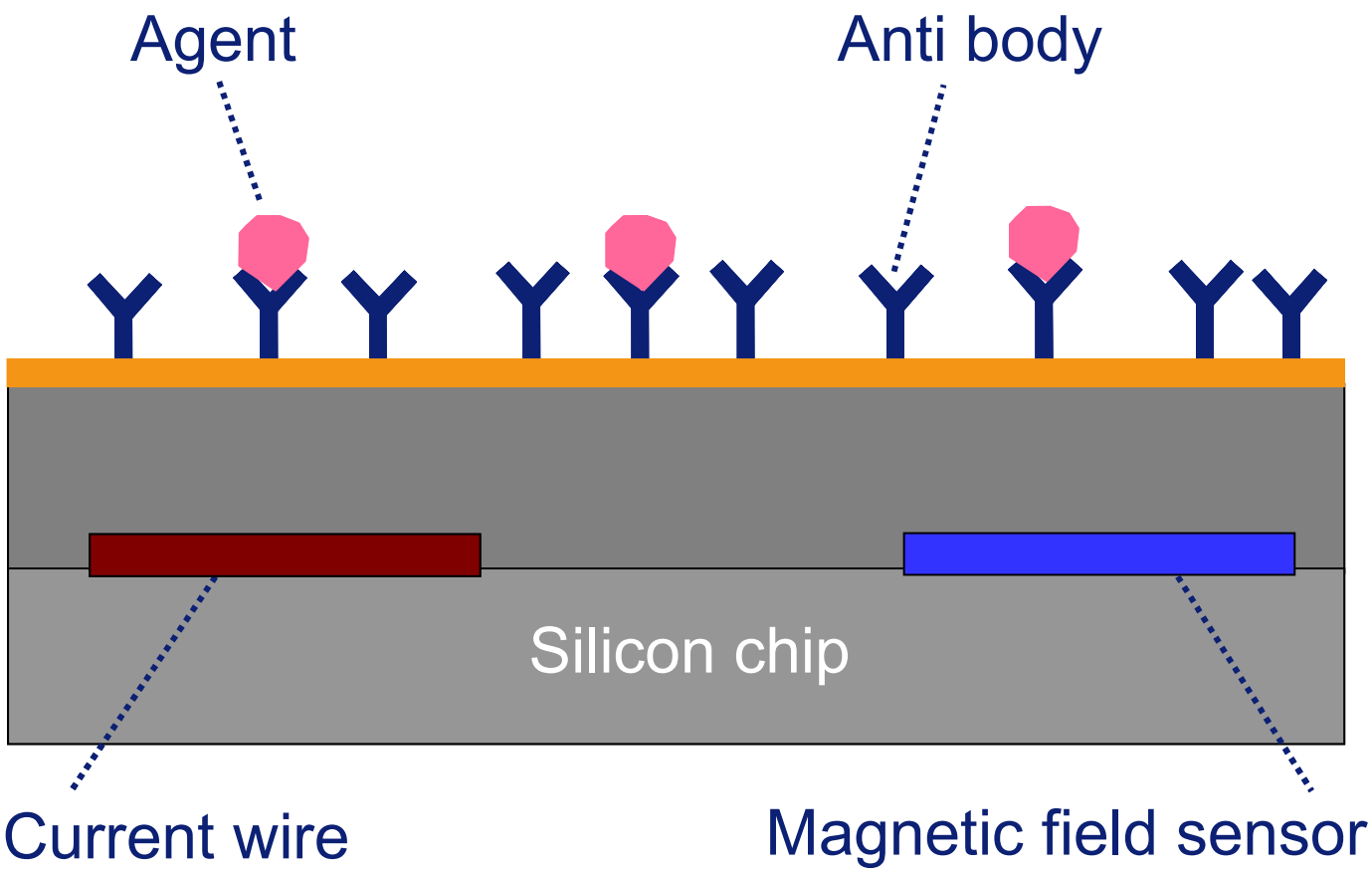

# **biosensors**
## bead attachment & measurement

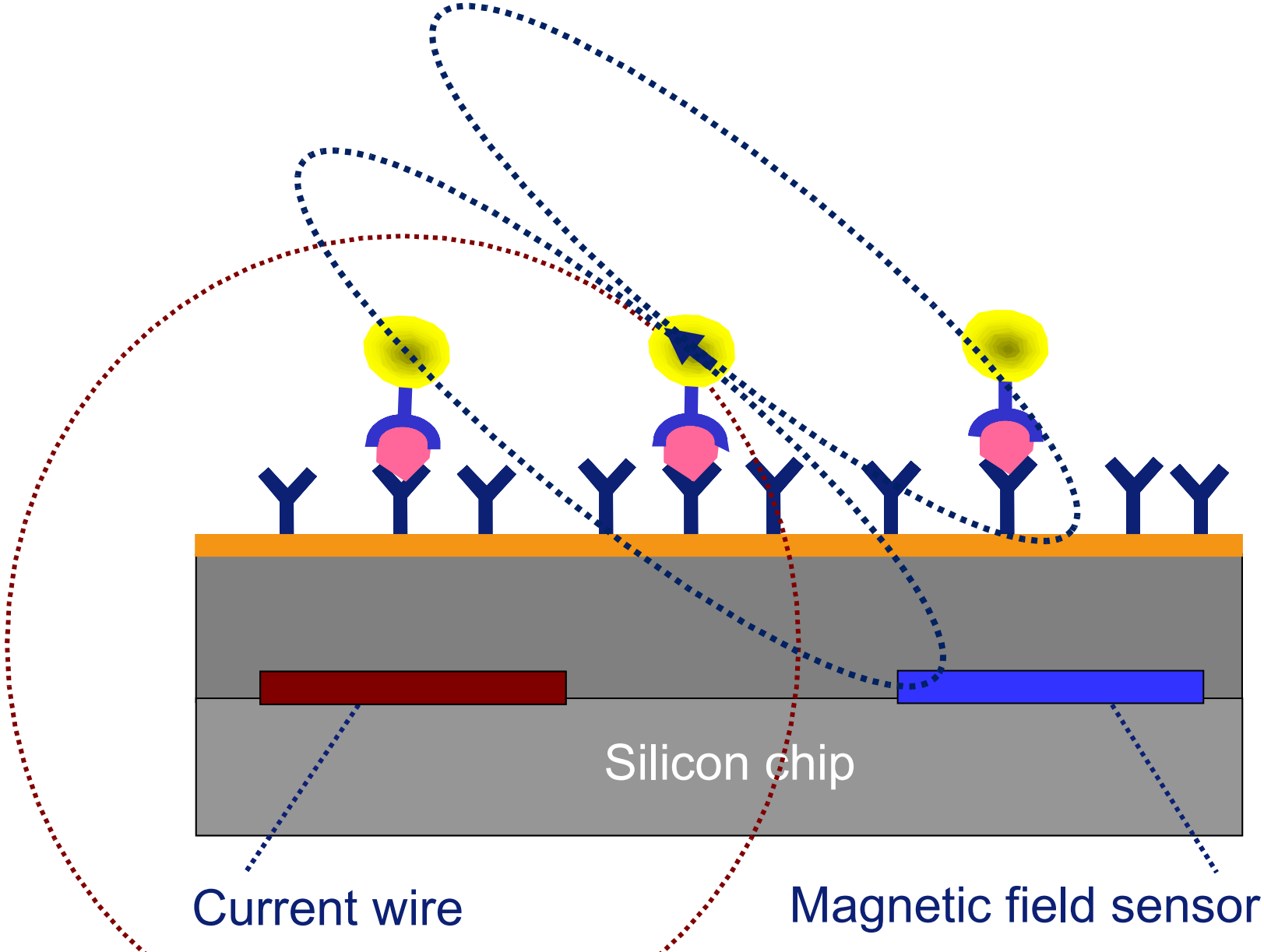

# **vortex switching**
# simulations

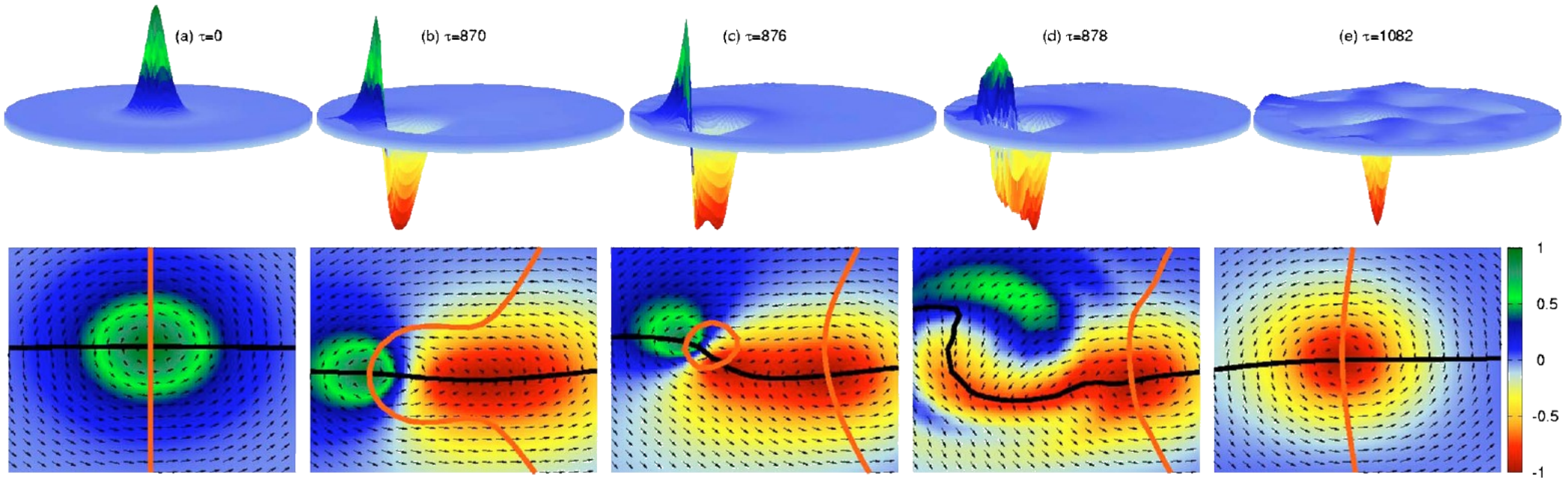


FIG. 1. (Color online) Time evolution of the vortex switching process from simulations: the top row shows the three-dimensional distribution of the magnetization $z$ component, the bottom row corresponds to the in-plane magnetization distribution near the vortex core. Isosurfaces $S_x=0$ (black curve) and $S_y=0$ (orange curve) are plotted to determine the vortex position. The current $j=-0.1$.

"Current induced switching of vortex polarity in magnetic nanodisks", Sheka et al., 2007. doi:10.1063/1.2775036

# **vortex switching**
# MFM measurements

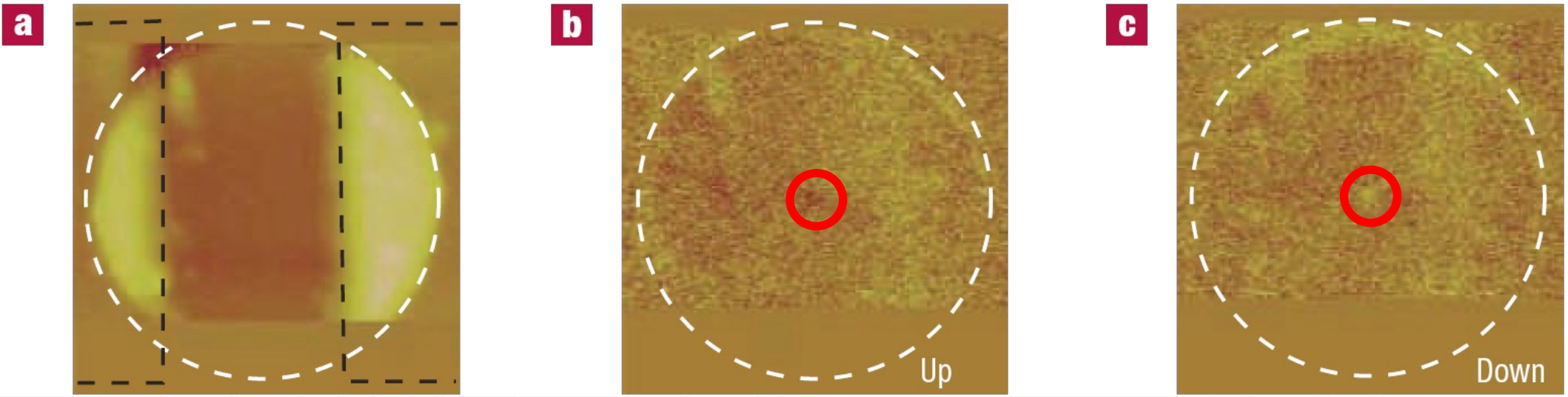


**Figure 3 MFM observation of electrical switching of the vortex core. a**, An atomic force microscopy image of the sample. A permalloy disk fills the white circle. The thickness of the disk is 50 nm and the radius is 500 nm. Two wide Au electrodes with 50 nm thickness, through which an a.c. excitation current is supplied, are also seen. **b**, MFM image before the application of the excitation current. A dark spot at the centre of the disk (inside the red circle) indicates that the core magnetization points upwards with respect to the paper plane. **c**, MFM image after the application of the a.c. excitation current at a frequency $f = 290$ MHz and amplitude $J_0 = 3.5 \times 10^{11}$ A m$^{-2}$ through the disk with a duration of about 10 s. The dark spot at the centre of the disk in **b** changed to a bright spot, indicating the switching of the core magnetization from up to down. **d**–**l**, Further successive MFM images, following those in **b** and **c**, with excitation current applied similarly between consecutive images. The switching of the core magnetization occurs from **b** to **c**, from **f** to **g**, from **h** to **i**, from **i** to **j** and from **k** to **l**. The MFM scan area was limited by the experimental time, and the parts of the sample that are not necessary to determine the core direction have been omitted from the images. The low MFM contrast for the core is due to the height difference between the disk and the electrodes.

"Electrical switching of the vortex core in a magnetic disk", Yamada et al., 2007. doi:10.1038/nmat1867

- the end -